# Research on Flare Burner for Venting in Gas Transmission Station

Xiangmin Dong [1,2,*], Nanxi Zhai [1], Xuan Liu [1], Qin Zhang [1,2], and Weihao Li [1,2]

[1] Beijing Gas Group Co., Ltd, 100035, Beijing, China;

[2] National Urban Gas Flow Measurement Station, 100035, Beijing, China.

* 1113617476@qq.com

**Abstract.** With the widespread application of natural gas, the venting of remaining natural gas is an issue that cannot be ignored. Direct venting causes serious environmental pollution, so thermal venting, also known as combustion venting, has become an important way to solve environmental pollution problems. This simulation first established two different types of burners, cluster and array, to quantitatively analyze the flame combustion characteristics. It simulated the distribution patterns of velocity, temperature, and key component concentrations of the two burners under the same number of holes and fuel flow rate. The research results indicate that due to the existence of oblique jet flow in the converging and array types, a reflux zone is formed at the outlet of the diffuser, and natural gas and air are mixed more thoroughly, resulting in a more stable flame. By comparing the burnout rate and combustion failure rate of the two types of burners, it was found that the convergent flame height and residual natural gas content during combustion were the lowest, resulting in better combustion efficiency. On this basis, while ensuring the same flow rate, the number of converging combustion holes was increased, the model parameters were improved, and it was found that the flame height was further reduced. At the same time, while maintaining the combustion removal rate, the burnout rate was improved. The development of the above-mentioned flare burner is of great significance in improving combustion efficiency, reducing flame height, and reducing environmental pollution caused by venting.

**Keywords:** station venting; Numerical simulation; Natural gas release.

## 1. Introduction

The greenhouse effect is one of the environmental issues that people have been paying close attention to in recent years, and it is the main factor causing global warming. In the industrial production process, the large amount of carbon dioxide and water generated by the combustion of fossil fuels entering the atmosphere changes the original composition of the atmosphere, disrupts the thermal balance of the natural greenhouse effect, and leads to intensified global warming. With the development of natural gas in urban pipelines, the issue of natural gas venting during the construction, operation, and maintenance of gas pipelines has attracted considerable attention, especially during the maintenance and repair process of gas pipelines [1-2]. Methane, as the main component of natural gas, has a global warming potential 34 times that of carbon dioxide after direct release, and its impact on the greenhouse effect is more severe [3-5]. In 2013, Aniefiok [6] indicated that direct or combustion emissions from venting systems may cause thermal and environmental pollution, exacerbating the greenhouse effect. In 2015, Zhang Wenli [7] analyzed and calculated variables such as pressure and venting volume during natural gas pipeline transportation through ignition and direct venting. In 2019, Baigmohammadi [8] conducted experimental and numerical studies on the mixed combustion of methane with air and hydrogen, and found that hydrogenation is an effective method to expand the flame existence limits of various flames in small combustion chambers. Most of the research on torch venting in China focuses on simulating the effects of different flow rates and the addition of different types and proportions of gases on torch combustion, with little attention paid to the model of torch burners leading to changes in the combustion efficiency of the venting torch. This article uses ANSYS Fluent software to model the natural gas flare burner and study the impact of different burner models on combustion efficiency. The analysis is conducted from the aspects of flow field, temperature field, and key component concentration field, and the simulation results are compared to develop an efficient, clean, and short flame flare burner. This work has important engineering practical value and theoretical guidance for natural gas combustion and venting.

## 2. Calculation model and boundary conditions

### 2.1 Calculation area model

Based on the actual operational data of the venting site, establish a physical model of the venting burner and the calculation area. The calculation area for thermal venting simulation calculation is shown in Figure 1, with a main diameter of D=4000mm, a height of H=11000mm, an outlet diameter of D1=2000mm, and a venting capacity of $840\,\mathrm{m}^3/h$. The layout of the two types of burners is shown in Table 1, and the structural schematic diagram is shown in Figures 2 and 3.

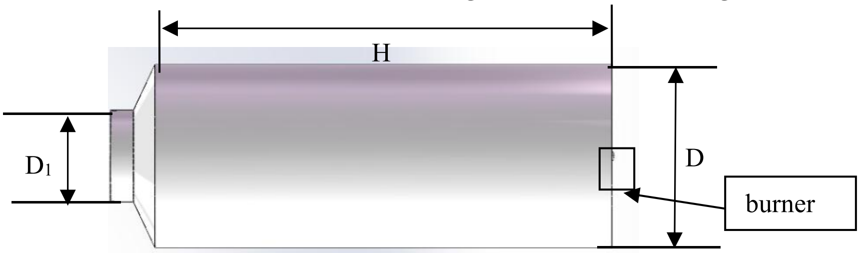


Fig. 1 Thermal venting simulation calculation model

Table 1. Two types of vent burner structures

| Burner model | Bore diameter | Layout situation |
|---|---|---|
| Convergent type | 10mm | Four combustion holes are arranged on a single combustion cylinder, with two on each horizontal and diagonal section, |
| Array type | 10mm | Eight branch array pieces are arranged at the top, with the array pieces forming a 45 degree angle, and four equally spaced combustion holes are arranged on each branch array piece |

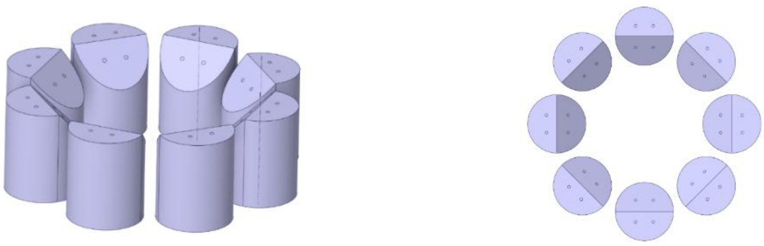

(a) Overall diagram (b) vertical view

Fig. 2 Schematic diagram of Convergent type vent burner

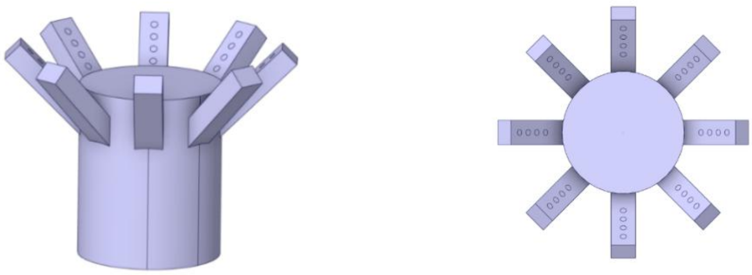

(a) Overall diagram (b) vertical view

Fig. 3 Schematic diagram of array type vent burner

### 2.2 Grid settings

In order to improve the accuracy of simulation calculations, unstructured grids were used to divide the model into grids, as shown in Figure 4. The methane concentration trends under 78000, 83000, 89000, and 100000 grid numbers were compared, and the calculation results showed little difference. However, there was a certain degree of difference between 89000 and 100000 grids. To ensure quality, 83000 grids were selected for simulation calculations.

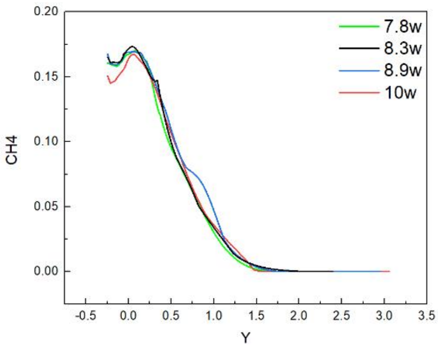


Fig. 4 Methane concentration distribution along the central axis under different grid numbers

### 2.3 Boundary condition

During the calculation process, a Fluent solver was used, combined with previous research experience and flow patterns [9-13]. Finally, the RANS standard k-ε turbulence model was chosen to simulate the turbulence process, a non premixed model was used to simulate the combustion process, a DO radiation heat transfer model was used to simulate the heat transfer process, and the SIMPLE algorithm was used to solve the pressure velocity coupling problem in the numerical simulation process, ensuring the accuracy of the calculation process.

## 3. Comparative analysis of different venting burners

### 3.1 Comparison of velocity distribution at the outlet of the venting burner

The flow rates of the two models are consistent, ensuring that their aperture and total number of holes are the same, so that the injection speed of the released air at the burner outlet is the same. As shown in Figure 5, for the convergent and array types, due to the presence of oblique jet flow, the released air will generate turbulence with each other. After leaving the burner, a reflux zone is formed at the outlet. The presence of the reflux zone can prolong the time the released air stays at the bottom of the combustion chamber, which helps to stabilize the bottom flame.

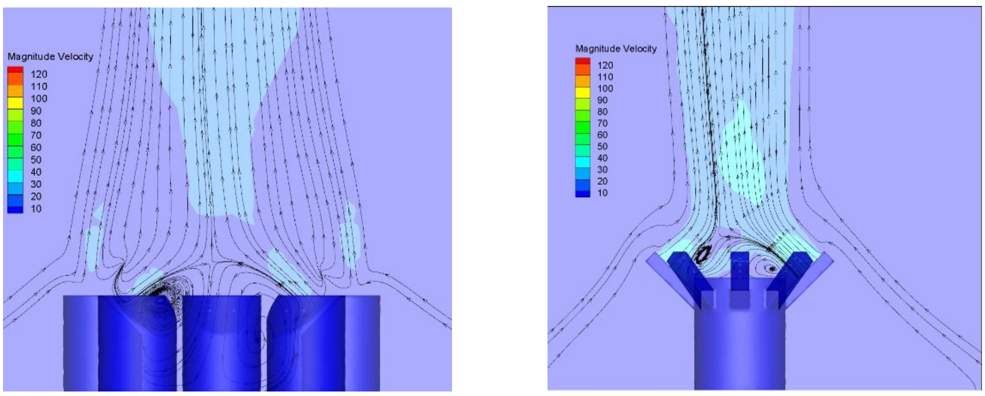


(a) Convergent type (b) Array type

Fig. 5 Velocity distribution diagram at the outlet of the venting burner

### 3.2 Comarison of temperature distribution in the venting space

As shown in Figure 6, the flame lengths of both models are around 4 meters. The center flame temperature of the convergent type venting burner model is the highest. This is because the ignition of natural gas after venting will generate a non free jet diffusion jet flame. When the jet flame can receive timely oxygen supplementation, the combustion reaction rate is faster, the combustion is more complete, the flame temperature is higher, and there will be no large amount of smoke, On the contrary, when oxygen cannot be replenished in a timely manner, combustion is insufficient, combustion is slower, flame temperature is lower, and a large amount of smoke is generated. As shown in Figure 7, temperature distribution above 500K can be observed. The highest temperature of the flames in both models is around 1900K-2000K, and the highest temperature of the convergent venting burner is slightly higher than that of the array burner. This is because the central area of the convergent venting burner is filled with smoke after combustion, So the temperature of the central axis at its bottom has also reached a very high level.

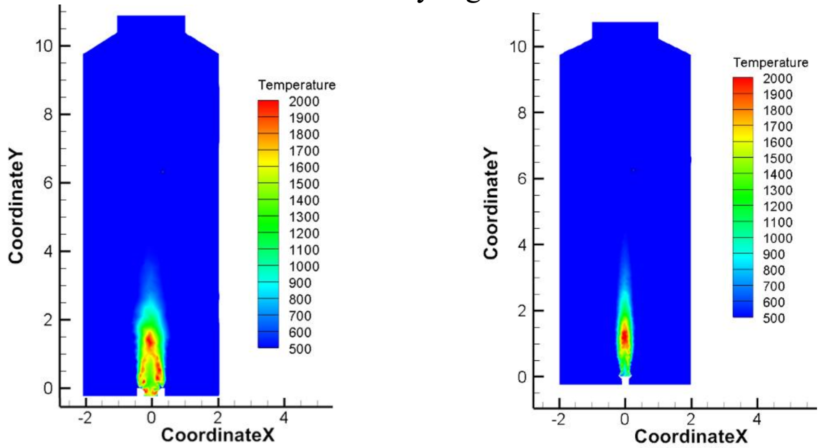


(a) Convergent type (b) Array type

Fig. 6 Temperature distribution map in the vent space

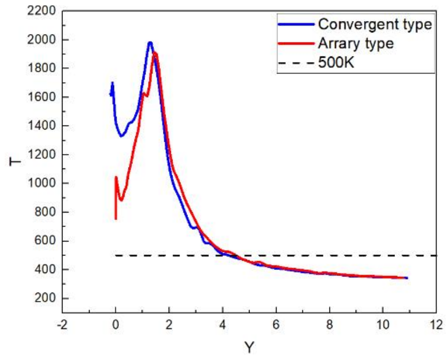


Fig. 7 Temperature distribution on the central axis of the venting burner

### 3.3 Distribution of component concentration at the outlet of the venting burner

As shown in Figure 8, after the array type release air is ejected, the release air can be partially mixed with oxygen, and then accumulate in the middle, forming local convection in the center, with more methane remaining in the center; Compared to the array type, each convergent burner is distributed in a circular pattern around the center. Therefore, after the release of air, compared to the first two models, it has a longer mixing time with oxygen, a longer flow development distance, and a larger reflux area. As the flow continues to develop upwards, methane gradually comes into more complete contact with oxygen, and methane burns completely, gradually reducing its concentration to 0.

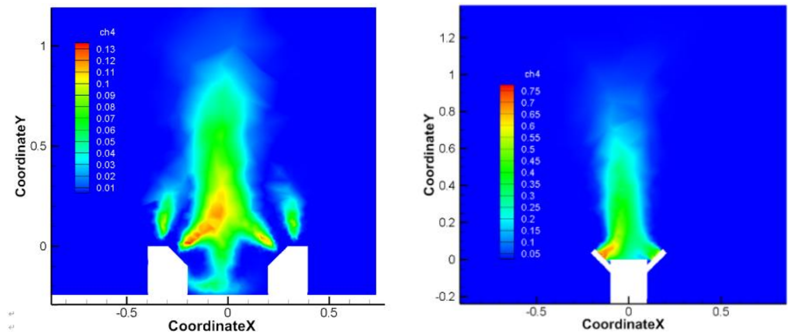


（a） Convergent type （b） Array type

Fig. 8 Methane concentration distribution at the outlet of the venting burner

Figure 9 shows that the production of carbon dioxide, a combustion product, is mainly in the center of the flame, which is the natural gas combustion area. Due to the high combustion temperature and oxygen concentration, when the inner air volume is lower than the required air for natural gas, it is in a lean burn state, resulting in a relatively low carbon dioxide content.

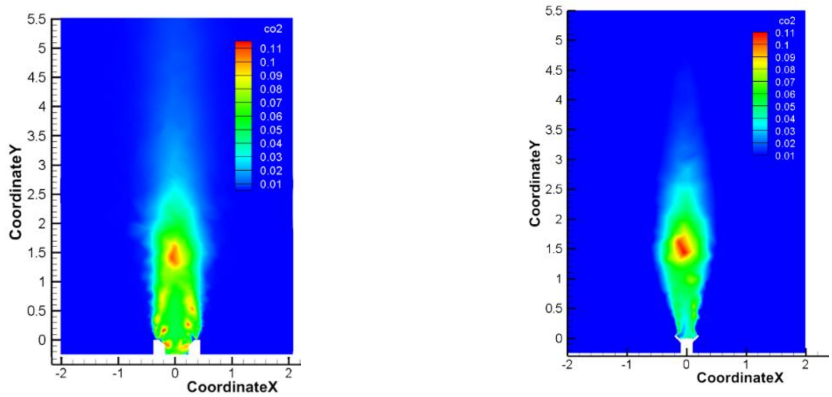


（a） Convergent type （b） Array type

Fig. 9 Carbon dioxide concentration distribution at the outlet of the venting burner

### 3.4 Comparison of combustion efficiency

At present, the national torch related standards in China mainly focus on the conventional process design of torches, and the emission control points only qualitatively specify the full combustion and flame monitoring of torches. Combustion efficiency is one of the most important parameters of torches, and low combustion efficiency can cause environmental pollution. In severe cases, it can form flammable and toxic atmospheres, causing personnel and property losses. There are two main indicators to measure the efficiency of torch combustion: Combustion Efficiency (CE) and Construction and Removal Efficiency (DRE) [14]. The burnout rate (CE) refers to the proportion of fuel completely converted to CO2 in the torch gas,The combustion failure rate (DRE) represents the proportion of fuel gas decomposition and damage in the torch gas.

The combustion failure rate is required to be above 98%, as shown in Table 2. The combustion failure rates of both burner models meet the requirements. In terms of burnout rate, the Convergent style has a slightly higher burnout rate than the array type.

Table 2. Burnout rate and combustion failure rate of two types of burners

| Burner model | CE | DRE |
|---|---|---|
| Convergent type | 71.91% | 99.94% |
| Array type | 68.57 | 99.84% |

# 4. Structural optimization of convergent type burners

By comparing the flow field, temperature field, distribution of key component concentration field, and combustion efficiency of the two models, it was found that the combustion degree of the convergent divergent burner was the most comprehensive, and the flame length was also relatively stable. Therefore, it was decided to further analyze and study the structure of the convergent divergent burner.

## 4.1 Model structure comparison

The original arrangement of 4 combustion holes on a single pipe has been optimized to include 8 combustion holes on a single pipe. The distribution of 8 pipes is still concentrated around the center, as shown in Figure 10.

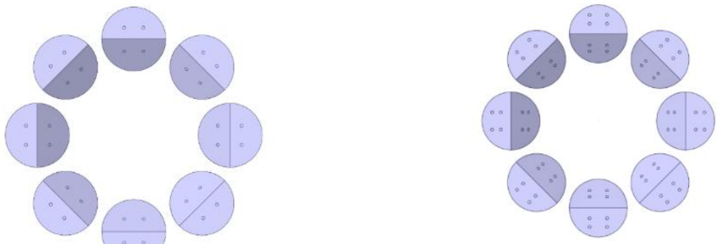

(a) Velocity streamline cloud map of 4 combustion holes in a single pipe (b) Velocity streamline cloud map of 8 combustion holes in a single pipe

Fig. 10 Model structure comparison diagram

## 4.2 Comparison of hole numbers with different distributions

As shown in Figure 11 (a) and (b), there are 8 circular distribution pipes. (a) There are two combustion holes on the horizontal top and slope of a single pipe, totaling four. (b) There are four combustion holes on the horizontal top and slope, totaling eight. From the velocity streamline cloud map, it can be seen that under the same flow rate, as the number of combustion holes arranged increases, the flow velocity at the burner outlet decreases and the disturbance of turbulence decreases, At the same time, it makes the reflux zone brought by the oblique jet more uniform and symmetrical.

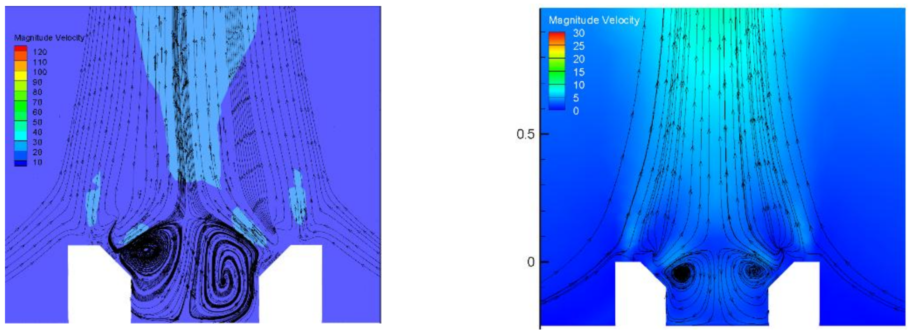


(a) Velocity streamline cloud map of 4 combustion holes in a single pipe (b) Velocity streamline cloud map of 8 combustion holes in a single pipe

Fig. 11 Velocity streamline cloud diagram of different combustion hole numbers

As shown in Figure 12 (a) and (b), the temperature cloud maps of the distribution of combustion holes 4 and 8 show that with the increase of the number of combustion holes, the highest temperature of the flame slightly increases, and the central high-temperature area is more uniform. The temperature at the bottom of the burner is reduced, which plays a certain protective role in the service life of the burner. As shown in Figure 13, the position of the central axis and the temperature curve under different numbers of combustion holes can be seen, The flame length has been reduced from 4m to 3.4m, with a 15% reduction in flame length. The flame length has been greatly reduced, and compare it with the flame length of 1250 $m^3/h$ at the East China Sea Octagonal Pavilion through conversion

 

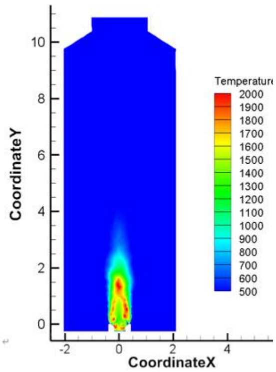


(a) Velocity streamline cloud map of 4 combustion holes in a single pipe

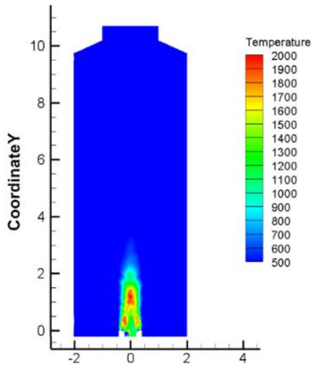


(b) Velocity streamline cloud map of 8 combustion holes in a single pipe

Fig. 12 Temperature cloud map of different combustion holes

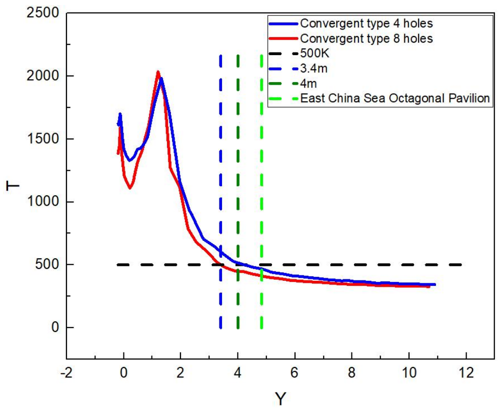


Fig. 13 Central axis position and temperature curve under different combustion hole numbers

As shown in Table 3, the optimized model increased the number of combustion holes. Although the combustion failure rate slightly decreased, it still met the standard. At the same time, compared with the original model, its burnout rate was improved and the flame length was reduced. Therefore, increasing the number of combustion holes helps to improve the combustion efficiency of the convergent burner.

Table 3. Burnout rate and combustion failure rate of the original model and optimized model

| Model | CE | DRE |
|---|---|---|
| Single tube with 4 combustion holes | 71.91% | 99.94% |
| Single tube with 8 combustion holes | 76.35% | 99.89% |

## 5. Summary

In the increasingly urgent situation of natural gas venting, the research on methane thermal venting flares has become particularly important. Fluent software was used to simulate the natural gas release situation of different burner models under constant wind speed, and the flow law of natural gas and the distribution law of combustion diffusion of each component were studied. The main conclusions are as follows:

(1)We have established models of convergent and array venting burners. Under the same flow rate, natural gas inlet velocity, and constant number of combustion holes, through analysis of the velocity field, it is found that both convergent and array burners have oblique jet flow, forming a reflux zone in the middle region, which plays a role in stabilizing the flame and strengthening its mixing.

(2) In the temperature field, the temperature distribution of each model was divided and analyzed, and the flame length was around 4m; In the distribution of methane and carbon dioxide concentration fields, due to the enhanced mixing of oblique jets, there is a more uniform mixed combustion in non premixed combustion. At the same time, the presence of a recirculation zone

also plays a role in stabilizing the bottom flame. Compared to the array type, the central area of the convergent type has a larger flow mixing space and less methane residue, indicating that natural gas combustion is more complete. Finally, the convergent type burner has the best combustion efficiency, with the highest burnout rate and combustion failure rate, while the array type has a slightly lower burnout rate.

(3) The simulation results of the convergent burner were better, so it was optimized by increasing the original 4 combustion holes to 8. Compared with the convergent burner with 8 holes, the velocity flow field and reflux zone of the 8-hole convergent burner were more uniform. In the temperature field, the flame height was reduced from 4m to 3.4m, a decrease of 15%, and the flame length was reduced. At the same time, the burnout rate of the 8-hole convergent burner was increased by about 5%, reaching 76.35% compared to the burnout rate of the 4-hole burner, which was 71.91%. The combustion removal rates of both were 99%. Therefore, the combustion efficiency of the convergent burner with 8 holes was optimized

## References

[1] Zhang Hui. Research on the Integrated Utilization Technology of Pressure Energy in Natural Gas Pipeline Networks [D]. Guangzhou: South China University of Technology, 2014.

[2] He Dong Bo, Jia Cheng Ye, Wei Yun Sheng, et al. The Situation and Development Trends of the World Natural Gas Industry [J]. Natural Gas Industry, 2022, 42 (11): 1-12.

[3] Liu Shu Le, Yan Wei, Gao Qing Xian, et al. The green-house effect of methane emissions from animal hus-bandry in China from a dual perspective [J/OL]. Envi-ronmental Science: 1-12 [2023-10-21]. DOI: 10.13227/j.hjkx.202212226.

[4] Szopa S, Naik V, Adhikary B, et al. Climate Change 2021: The Physical Science Basis. Contribution of Working Group I to the Sixth Assessment Report of the Intergovernmental Panel on Climate Change [R]. Cam-bridge, United Kingdom and New York, USA: Cam-bridge University Press, 2021.

[5] IPCC. Summary for policymakers[M]. Climate change 2013:The physical science basis. Contribution of work-ing group I to the fifth assessment report of the inter-governmental panel on climate change, Cambridge: Cambridge University Press, 2013.

[6] Aniefiok E. Gas Flaring and Venting Associated with Pe-troleum Exploration and Production in the Nigeria’s Ni-ger Delta[J]. American Journal of Environmental Protec-tion，2013(4): 70-77.

[7] Zhang Wen Li. Research on the design method of vent pipes in natural gas transmission pipelines [D]. Cheng-du: Southwest Petroleum University, 2015.

[8] Baigmohammadi M, Tabejamaat S, Yeganeh M. Experi-mental study of methane-oxygen premixed flame char-acteristics in non-adiabatic micro-reactors[J]. Chemical Engineering and Processing-Process Intensification, 2019, 142: 10.

[9] Jiang Jie Yu, Li Hong Xu, Sui Chun, et al. Analysis of flow field transport characteristics of hydrogen non premixed combustion [J]. Combustion Science and Technology, 2020, 26 (2): 146-154.

[10] Yu Qiao Yan, Hou Lei, Chai Chong, et al. Research on the length and damage range of jet flames in high-pressure natural gas pipelines [J]. Petroleum Science Bulletin, 2022, 7 (4): 593-603.

[11] Ali A, Alaleh B H A, Hadi M S, et al. CFD simulation of an industrial steam methane reformer: Effect of burner fuel distribution on hydrogen production[J]. Fuel, 2023, 352.

[12] J.H. M R,S. O M,H. N A, et al. Cooling a cavity equipped with a hot electrical element using nano-encapsulated phase change material /water: Study of mixed convection and natural convection[J]. Case Stud-ies in Thermal Engineering, 2023, 50.

[13] Qi Sheng, Li Xiang. Numerical simulation of biomass gas combustion and NO generation in a gas furnace blended combustion [J]. Natural Gas Chemical (C1 Chemistry and Chemical), 2021,46 (5): 112-117.

[14] Wang Zhen Dong, Shen Xiao Bo, Xiu Guang Li, et al. Research on Control Standards and Regulations for Torch Pollution in the Petrochemical Industry at Home and Abroad [J]. Environmental Science Research, 2019, 32 (9): 1456-1463.

[15] Wang Dong Bao, Kuang Xiao Feng. Computational flu-id dynamics simulation of the thermal radiation intensi-ty of the Bajiaoting platform flare [J]. China Offshore Oil and Gas, 2005 (5): 70-74.